Eight Kilowatt Hall Thruster System Characterization

IEPC-2013-317

Presented at the 33rd International Electric Propulsion Conference,
The George Washington University • Washington, D.C. • USA
October 6 – 10, 2013

James Szabo,[1] Bruce Pote,[2] Lawrence Byrne,[3] Surjeet Paintal,[4] Vlad Hruby,[5] Rachel Tedrake,[6] George Kolencik,[7] Chas Freeman[8]
Busek Co. Inc, Natick, MA, 01760, USA

Nikolaos Gatsonis[9]
Worchester Polytechnic Institute, Worcester, MA 01609, USA

Abstract: A nominal 8-kW Hall thruster system was developed for high power spacecraft applications. This thruster is supported by a 1.3 cm hollow cathode. Performance was measured directly at conditions representative of the space environment, bringing the Technology Readiness Level (TRL) to 5. At nominal conditions, the thruster delivers half a Newton of thrust at 8-kW with a specific impulse of greater 1900 s. Deep throttling capabilities were demonstrated. Performance and throttling curves are presented. Data were taken with xenon, krypton, and iodine. Details of the thruster and system components are also presented.

Nomenclature

$\vec{B}$	=	magnetic field
D	=	thruster diameter
$\vec{E}$	=	electric field
I_d	=	discharge current
I_{sp}	=	specific impulse
$\dot{m}$	=	mass flow rate, subscripts a for anode
P	=	power, subscripts d for discharge, n for nominal
T	=	thrust
V_d	=	discharge potential
v	=	velocity
η	=	efficiency, subscript t for thrust

[1] Chief Scientist for Hall Thrusters, jszabo@busek.com
[2] Director, Hall Thrusters, bpote@busek.com
[3] Senior Bus and Payload Engineer, larry@busek.com
[4] Research Engineer, spaintal@busek.com
[5] President, vhruby@busek.com
[6] Research Engineer, rachel@busek.com
[7] Research Engineer, george@busek.com
[8] Laboratory Manager, cfreeman@busek.com
[9] Professor, Mechanical Engineering Department, gatsonis@wpi.edu

I. Introduction

THE Hall Effect Thruster (HET) is an efficient form of electric space propulsion that is typically used for orbit-raising and orbit maintenance. This paper reports the Busek BHT-8000, a thruster sized to operate at 8 kW. This thruster is supported by a 1.3 cm hollow cathode. The BHT-8000 has been tested with a variety of propellants including xenon, krypton, and iodine.

Hall thrusters were invented in the United States[1, 2, 3] but the first to fly in space was a Stationary Plasma Thruster (SPT) launched in 1971 aboard the Soviet Meteor-18 spacecraft.[4] The first American designed HET to fly in space was the Busek BHT-200[5], launched in 2006 as part of the US Air Force TacSat-2 satellite and fueled by xenon (Xe). The nominal operating power was 200 W. The BHT-8000 was designed to operate at 8000-W, a factor of 40 increase with respect to the BHT-200. Other high technology readiness level (TRL) Busek thrusters of a similar design include the BHT-600,[6] BHT-1000,[7] BHT-1500,[8] and BHT-20K.[9] These thruters operate at nominal power levels of 600-W, 1.0-kW, 1.5-kW, and 20-kW, respectively.

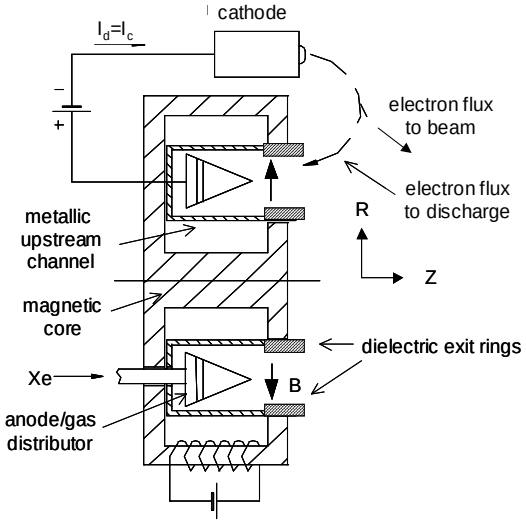

Figure 1. Nominal axisymmetric Hall Effect Thruster geometry.

A Hall Effect Thruster uses crossed electric and magnetic fields to generate and accelerate ions. The gas in the discharge is partially ionized, although propellant utilization may approach 100%. The peak electron temperature is typically below several tens of volts. Figure 1 is an approximate representation of the BHT-8000 geometry. The overall structure is defined by a magnetic circuit that produces a steady magnetic field, $\vec{B}$, in the nominal radial direction across an annular channel. The upstream portion of the channel is metallic (the outer anode). Neutral propellant is introduced through a metallic gas distributor inside the annulus (the inner anode). Together, the metallic upstream channel and gas distributor form the anode assembly. The downstream portion of the channel is formed by dielectric material, between which the bulk of the plasma discharge occurs. A potential difference or discharge voltage, V_d, is applied between the anode assembly and a hollow cathode located outside the channel. The resulting electric field, $\vec{E}$, is predominantly axial and is concentrated near the channel exit by interactions between the magnetic field and the plasma. The cathode is allowed to float with respect to facility ground.

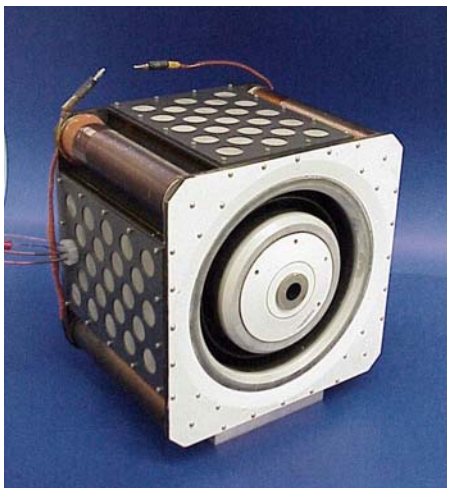

Figure 2. The BHT-8000 thruster.

In the channel, electrons are strongly magnetized and their transport is predominantly azimuthal due to the $\vec{E}\times\vec{B}$ Hall Effect. The extended electron path enables an efficient, impact driven ionization cascade. Axial transport across $\vec{B}$ is provided by collisions, wall effects, and additional, "anomalous" transport identified in the early 1960s.[10] Ions are weakly magnetized and most are accelerated directly out of the channel, forming the ion beam. The bulk of the cathode electrons go to neutralize the ion beam current, I_b. However, some circulate back through the channel, driven by the potential difference. These electrons seed the discharge cascade. A control volume analysis shows that the discharge current is equal to the cathode current.

II. Apparatus and Procedure

The BHT-8000 is a single stage Hall thruster designed to operate at discharge power levels of 2 to 10-kW and discharge potentials up to 700-V. The original thruster, Version 1, was built in the late 1990s.[11] The Technology Readiness Level[12] or TRL of the present thruster, Version 2, is estimated at 5. Figure 2 shows the BHT-8000 Version 2 (hereafter referred to simply as the BHT-8000) on the bench. The mean diameter of the discharge cavity is

170-mm. The discharge channel exit rings are made of boron nitride. The hollow cathode may be mounted along the geometrical thruster axis, a location shown to reduce beam divergence[13,14] and maximize thrust efficiency. Electrical isolation of the anode from the propellant line is achieved with a custom high voltage ceramic break.

With reference to Figure 1, which is not to scale, the outer anode assembly passively shunts a portion of the magnetic field, creating a magnetic lens with a steep axial gradient in $|B|$ and near zero $|B|$ close the anode.[15] This method of shaping the magnetic field is different from the magnetic "screens" used in the SPT-100, for instance.[16] The magnetic lens concept itself was first described in the 1960s.[17,18] Trim coils co-located with the anode assembly may be used to actively shunt an additional portion of the magnetic flux to "focus" or optimize the lens. Active shunting improves thrust efficiency at some flow rates and discharge voltages.

The hollow cathode design is scaled from the BHC-1500, a low current cathode which was flight qualified and demonstrated on orbit with the BHT-200 Hall thruster on the TacSat-2 mission. Busek's design uses a porous tungsten hollow insert impregnated with a low work function emitter comprised of a barium-calcium-aluminate mixture. A co-axial tantalum swaged heater wire is used to bring the emitter to the operating temperature range, 1000-1200°C. The cathode keeper that surrounds the emitter is used to start the cathode and sustain an internal discharge before establishing thruster operation. The keeper also provides a radiation and sputter shield to protect the emitter and heater from environmental damage. Operating conditions are dependent upon the required current and thruster flow rate. The flow rate of propellant is typically 4 - 10% of the anode mass flow rate. Figure 3 shows the 1.3-cm cathode currently used with the BHT-8000.

Figure 3. Busek's 1.3-cm hollow cathode.

To accurately measure performance, the background pressure must be low enough that it does not significantly affect the plasma processes or feed the discharge background neutrals. To achieve such a space-like environment, the BHT-8000 was tested with xenon in Busek's cryo-pumped T8 vacuum chamber, shown in Figure 4 (left), which has a nominal Xe pumping speed of 200,000-l/s. This facility has a diameter of 2.4-m and a length of 5-m. Background pressure was measured with an ion gauge located on the wall of the facility. Krypton testing also took place in the T8 facility. Additional xenon testing focused on plume analysis was conducted at the Jet Propulsion Laboratory in 2005. That testing is described fully in Ref. 13. Iodine performance testing took place in Busek's 1.8-m diameter T6 facility.

At Busek, the discharge was powered by a 730-V, 55-A power supply allowed to float with respect to facility ground. A 40-μF capacitor bank was typically placed in parallel with the discharge to filter oscillations. The inner and outer solenoid circuits were driven by separate DC power supplies independent of the discharge. Trim coils were driven by an additional power supply. Figure 4 (right) is a nominal power supply diagram.

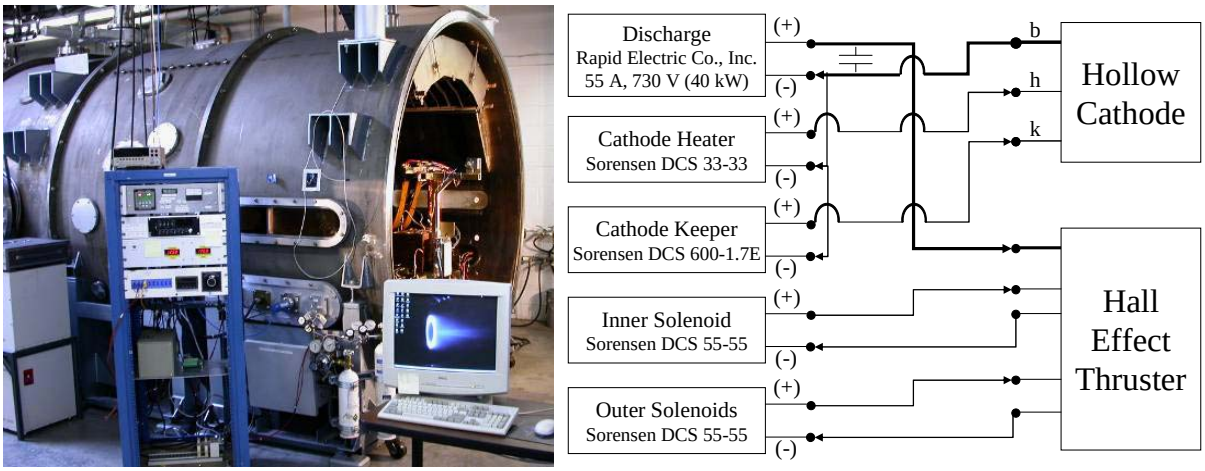

Figure 4. T8 test facility and nominal power supply diagram.

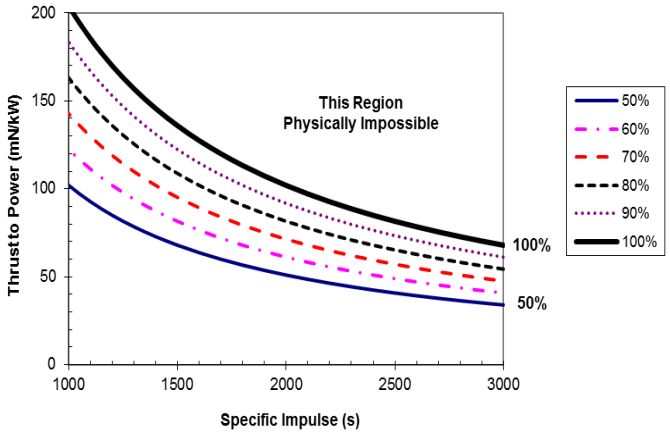

Figure 5. Relationship between thrust to power, specific impulse, and efficiency.

At Busek, thrust, T, was measured directly with an inverted pendulum, "Null" type thrust stand that is corrected for thermal drift.[19] Xenon and krypton were fed with a calibrated feed system based upon Commercial Off-The-Shelf (COTS) mass flow controllers. Iodine was provided by a custom feed system based upon the sublimation of iodine crystals in a reservoir located outside of the test chamber.[20,21]

Specific impulse, I_{sp}, is determined from thrust and mass flow rate, $\dot{m}$, by the equation

$$I_{sp} = T/\dot{m}g_0 \,. \quad (1)$$

Here, g_0 is the force of gravity on the surface of Earth. Anode I_{sp} is calculated using only anode flow rate, $\dot{m}_a$. Efficiency is determined from T, $\dot{m}$, and the power provided to the thruster, P, through the equation

$$\eta = T^2/2\dot{m}P \,. \quad (2)$$

In Equation 2, P includes the power provided to the discharge ($P_d = V_d I_d$), electromagnets, and cathode. At the system level, PPU losses would also be included. Efficiency and specific impulse are related to thrust to power by

$$T/P = 2\eta/I_{sp}g_o \,. \quad (3)$$

This relationship is plotted in Figure 5.

II. Results

Over the last decade, BHT-8000 has been extensively tested with a variety of propellants. During that time, the system has continually evolved toward a flight system. Key results are summarized in the following sections.

A. Baseline Xenon Performance

Figure 6 plots thrust against total specific impulse as the BHT-8000 is throttled between P =2-kW and P =8-kW. The discharge potential in this data set is V_d =200 to 400-V. Peak thrust exceeds half a Newton at I_{sp} = 1900-s. The cathode to anode flow ratio ($\dot{m}_c/\dot{m}_a$) for the data in Figure 6 was approximately 10%. Reducing this ratio increases total specific impulse and efficiency, as discussed in section II-b. The data show that the BHT-8000 throttles efficiently. At V_d = 300-V, the efficiency is 58% at 8-kW, 57% at 4-kW, and 54% at 3-kW. Table 1 is a basic throttle data corresponding to Figure 6. The thruster has also been tested at higher and lower discharge potentials. The chief benefits of higher voltage are increased specific impulse and efficiency. For example, at 8.8-kW and 600-V, I_{sp} = 2660-s and η =62%. At 9.1-kW and 700-V, I_{sp} = 3047-s and η =63%. The chief benefit of low voltage is high thrust to power. At P <2-kW and V_d <= 200-V, T/P can exceed 90-mN/kW.

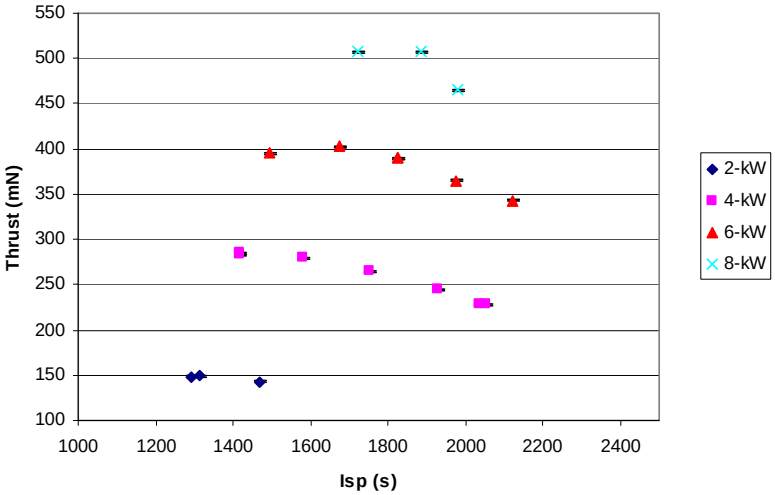

Figure 6. Thrust vs. Total I_{sp} at power levels of 2 to 8-kW.

Table 1. BHT-8000 throttle table.

DISCHARGE VOLTAGE (V)	THRUST (mN)	TOTAL POWER (W)	TOTAL ISP (S)	TOTAL EFFICIENCY (%)
NOMINAL DISCHARGE POWER 2000W				
200	149	2011	1293	0.47
250	143	2022	1470	0.51
NOMINAL DISCHARGE POWER 4000W				
200	285	4040	1416	0.49
250	279	3999	1578	0.54
300	265	3995	1752	0.57
350	245	4063	1927	0.57
400	228	4026	2052	0.57
NOMINAL DISCHARGE POWER 6000W				
200	395	6022	1492	0.48
250	403	6016	1674	0.55
300	390	6022	1826	0.58
350	365	5999	1977	0.59
400	343	6158	2123	0.58
NOMINAL DISCHARGE POWER 8000W				
250	508	8096	1722	0.53
300	507	8078	1884	0.58
350	465	8060	1979	0.56

The uncertainty associated with BHT-8000 performance measurements was estimated by standard methods.[22] Table 2 summarizes the calculation for P, T, $\dot{m}$, I_{sp}, and η. The normalized variance or uncertainty in P is estimated to be a negligible 1.1%. The uncertainty in T is estimated to be 2.1%. Contributions include the calibration curve, sample-to-sample signal variation, and thrust stand drift. The uncertainty in $\dot{m}$ is estimated to be 2.6%. Contributions include uncertainties in the flow controller and estimated propellant backflow from the test facility. The uncertainty in specific impulse is given by the equation

Table 2. Performance measurement uncertainty.

Figure of Merit	Constituent	Normalized Variance (%)
Power	Voltage	0.5
	Current	1.0
	Standard Dev. (RMS)	**1.1**
Thrust	Slope of calibration curve	0.5
	Sample to sample variation	0.5
	Signal drift	2.0
	Standard Dev. (RMS)	**2.1**
Mass Flow	Flow Controller	1.0
	Backflow	2.4
	Standard Dev. (RMS)	**2.6**
Efficiency	Standard Dev. (RMS)	5.1
Isp	Standard Dev. (RMS)	3.4

$$\left(\frac{\sigma_{I_{sp}}}{I_{sp}}\right)^2 = \left(\frac{\sigma_T}{T}\right)^2 + \left(\frac{\sigma_{\dot{m}}}{\dot{m}}\right)^2. \quad (4)$$

Given prior numbers, this yields uncertainty in I_{sp} of 3.4%. The normalized variance in efficiency, η, is given by

$$\left(\frac{\sigma_\eta}{\eta}\right)^2 = 4\left(\frac{\sigma_T}{T}\right)^2 + \left(\frac{\sigma_{\dot{m}}}{\dot{m}}\right)^2 + \left(\frac{\sigma_P}{P}\right)^2. \quad (5)$$

Given previous numbers, the normalized uncertainty in η is estimated to be 5%.

These uncertainties should be applied to the values in Figure 6 and Table 2**.** For instance, at V_d =400-V and P =6.2-kW, I_{sp} =2123-s +/- 72 s, and η =58% +/- 3%.

B. High Voltage Propellant Isolation

For $I_{sp} \geq 3000$-s, the required potential difference may be 700-V or higher. Electrical isolation of the anode from the propellant line is provided by a custom ceramic break developed by Busek. The voltage isolation provided by the break was measured in an experiment that also included two commercially available breaks. In all three isolators, a section of alumina is brazed to metal end-caps terminating in metal tubing. In the Busek isolator (Figure 7), the propellant flows through a molded alumina spiral. In the second isolator, provided by Insulator Seal Inc. (ISI), the propellant flows through a tube packed with alumina beads. In the third isolator, also provided by ISI, the propellant flows through an empty tube. Key dimensions of these three isolators are noted in Table 3.

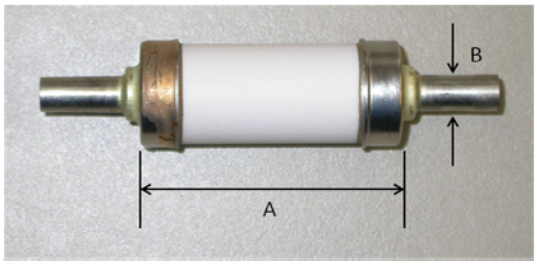

Figure 7. Busek's high voltage isolator.

Table 3. Propellant isolator dimensions.

Isolator	A [in]	B [in]
ISI Straight Isolator	0.85	0.125
ISI Beaded Isolator	1.07	0.125
Busek Spiral Isolator	1.5	0.25

The isolation experiment was conducted in the laboratory; external isolator surfaces were exposed to air at one atmosphere. Internal pressure was varied between 0 and 40-Torr, as measured with both a MKS Baratron pressure transducer (used exclusively for xenon) and an Omega high accuracy pressure sensor. A calibration curve between the two pressure transducers was obtained so that reported pressures were on the same scale. A potential difference across the isolator was applied with a Bertran High Voltage power supply.

The procedure was to straightforward. First, the propellant isolators were evacuated. Then they were incrementally pressurized. At each pressure, the potential difference was increased until the voltage collapsed.

With xenon, the Busek isolator provided approximately 4-kV of isolation across the tested pressure range. The beaded and straight isolators showed a much greater variation with pressure, with minimum breakdown voltages at 2-kV and 0.5-kV, respectively. The latter is higher than expected based upon Paschen breakdown data in the literature. The xenon data are plotted in Figure 8.

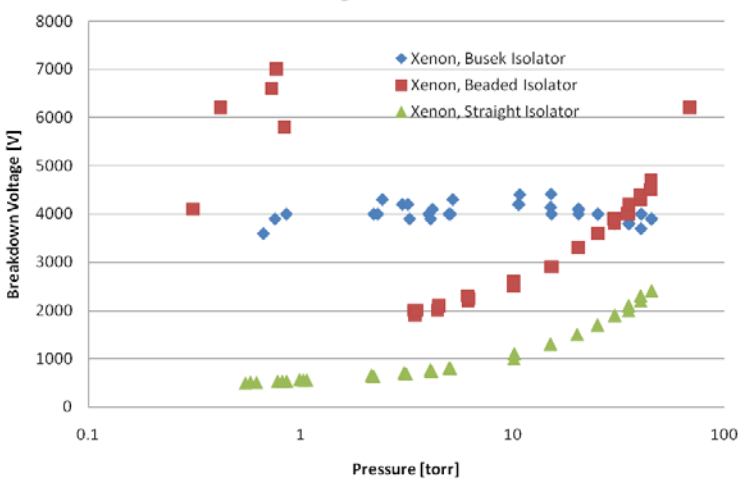

Figure 8. Breakdown voltage for xenon.

With iodine, Busek isolator provided at least 2.5- kV of isolation. With the beaded isolator, the minimum was approximately 1.5-kV. With the straight isolator, the minimum was again approximately 0.5-kV.

C. Trim Coils

One configuration of the BHT-8000 may be equipped with trim coils to change the amount of magnetic flux flowing through the anode shunt. Trim changes the magnitude and shape of the magnetic field in the channel. This can theoretically decrease the ion flux flowing into the discharge chamber walls, thereby increasing propellant utilization, efficiency, and lifetime.

Thrust measurements confirm that the trim coils can increase efficiency at some conditions. Table 4 shows the effect of trim at V_d =151-V, $\dot{m}_a$ =154-sccm, $\dot{m}_c$ =7.5-sccm with the current though the external solenoids fixed. Application of trim increased anode efficiency from 40% to 46 % At V_d =151-V, $\dot{m}_a$ =250-sccm, $\dot{m}_c$ =14-sccm, application of trim increased anode efficiency from 38% to 47%. Measured background pressure was 5.9-6.9 x 10^{-5}-Torr during these measurements. Error bars in thrust were several percent, which is not enough to account for the apparent improvement. Performance gains were smaller at V_d =300-V, $\dot{m}_a$ =154-sccm, $\dot{m}_c$ =7.5-sccm, where trim increased anode efficiency from 58% to 62%. No significant gains were observed at V_d =445-V.

Table 4. Effect of trim on efficiency at V_d~150 volts.

Trim [A]	Anode Efficiency [%]
0.0	40
1.0	44
2.0	46
3.0	45

D. Cathode Flow Rate

With the cathode mounted along the thruster axis, the cathode flow rate $\dot{m}_c$ may be less than 5% of the anode flow rate $\dot{m}_a$. Table 5 illustrates the effect of varying ($\dot{m}_c / \dot{m}_a$) upon upon cathode floating potential, specific impulse, and efficiency. The data were taken at V_d =300-V, $\dot{m}_a$ =154-sccm, with constant magnetic field. As $\dot{m}_c / \dot{m}_a$ decreases, total efficiency and specific impulse both increase. The effect of cathode flow rate upon emitter temperature and lifetime must also be considered when setting the cathode flow rate.

Table 5. Effect of cathode flow rate on specific impulse and efficiency at V_d=300-V.

Flow Ratio [%]	Floating Potential [V]	Total Isp [s]	Total Efficiency [%]
9.6	-11	1729	55.1
7.8	-12	1769	56.4
5.8	-13	1794	56.8
3.9	-16	1828	57.7

E. Plume Measurements

The most extensive plume survey of the BHT-8000 was conducted at JPL in 2005. Measurements included plume current, discharge current oscillations, and species fractions. The thruster was test with two cathodes; a JPL LaB_6 cathode was mounted to the side of the thruster, distal to the discharge region, and a Busek 1.3-cm barium-tungsten cathode was mounted along the axis of the thruster per the nominal design. Figure 9, taken at Busek, shows the region of the axial cathode exit with the thruster operating at P_d =6.5- kW and V_d =450-V. Here, the cathode was set back from the most forward plane of the thruster.

The test matrix at JPL extended from 2-kW to 8-kW and from 200-V to 500-V. Eight kilowatts was demonstrated at 200, 300, 400 and 500-V.

The most significant outcome of this testing may have been a series of plume current measurements that clearly showed beam divergence was lower cathode when the cathode was mounted along the axis.[13] Figure 10 plots the measured plume current at 8-kW, 300-V and 400-V. Complete details are found in Ref. 13. The background pressure was at or below 2 x 10^{-5}-Torr for this testing.

ExB probe measurements showed the Xe^+ ion species fraction was 94% to 95%, and the Xe^{2+} fraction was 5% to 6%. These were judged to be typical results for Hall thrusters operating at discharge voltages of 300-V to 500-V. No appreciable difference was observed with the distal JPL cathode.

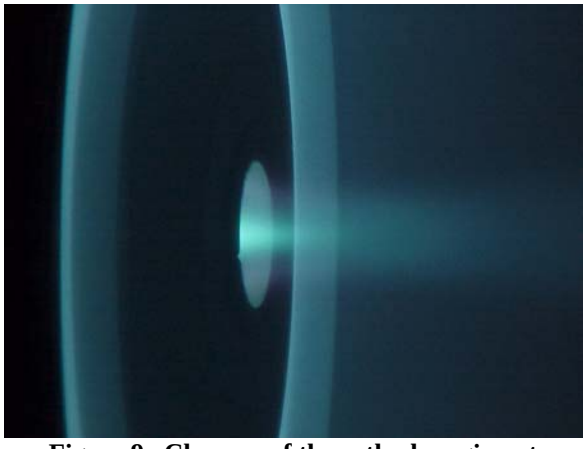

Figure 9. Close up of the cathode region at V_d=450-V and P_d=6.5-kW.

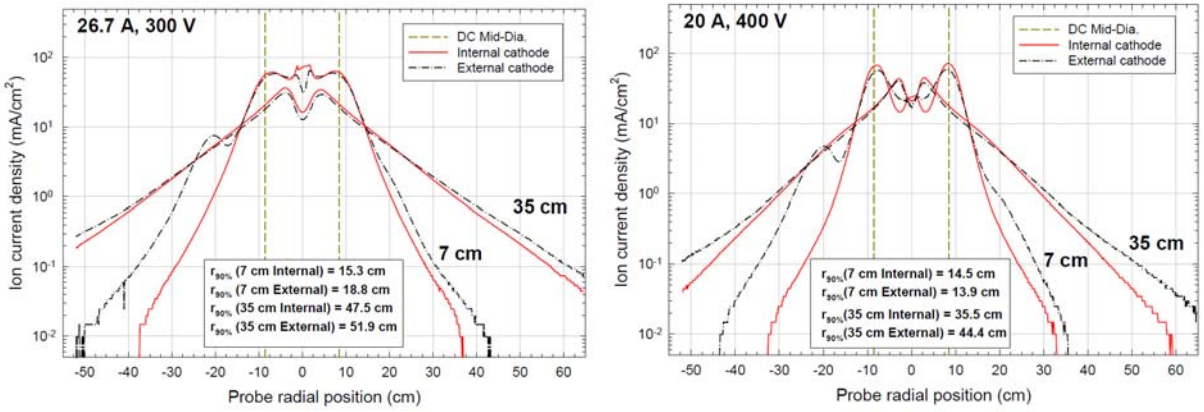

Figure 10. Current density vs. probe position with internal and external cathodes at V_d=300-V, P_d=8-kW.

F. Cathode Lifetime Estimate

The lifetime of the Busek 1.3-cm hollow cathode was predicted with a barium depletion model developed at WPI. The model is 1-D, with a variant emitter insert temperature profile and Ba/BaO axisymmetric vapor diffusion model based on the selected transport equations.

In Barium Calcium Aluminate impregnated tungsten emitters, barium is supplied to the tungsten surface by chemical reactions of the $BaO:CaO:Al_2O_3$ mixture. The key in the operation of the emitter is in achieving a barium-on-oxide monolayer that lowers the work function of the surface. The lifetime mechanism of barium-impregnated cathodes is determined by the transport of barium away from the insert. In hollow cathodes the emission of the Ba and BaO from the surface as well as the deposition of oxides is affected by the flow of xenon. The lifetime model developed captures the essential characteristics of the thermochemical processes of the barium diffusing through the porous insert and can be coupled to an insert-region flow model.

Table 6 Depletion time for the 1.3-cm cathode 6:1:2 insert.

EMITTER TEMP (°C)	TIME (hrs)
1250	2,040
1200	4,800
1150	12,000
1100	32,000
1050	92,000
1000	>100,000
950	>100,000

The computer simulation code implements the thermochemistry model of Lipeles and Kan[23] that provides the evaporation and depletion of BaO from a single pore. Under this model BaO is produced by the thermal decomposition of the impregnated material. For a given stochiometric composition of $BaO:CaO:Al_2O_3$ the phase compositions are calculated based on the phase diagram by Wolten.[24] BaO pressure is then used to calculate the gaseous barium pressure and effusion rate.

Both O-D and 1-D lifetime estimate models developed by WPI were applied to the 1.3-cm cathode. Typical measured emitter temperatures vary between 1250-C and 900-C and vary with operating conditions. This corresponds to a lifetime range of 2,040-h to greater than 100,000-h. Table 6 lists the predicted cathode lifetime from the 0-D model across the full range of temperatures.

G. Krypton Performance

The BHT-8000 has also been tested at power levels up to 6-kW with krypton propellant. The data clearly show that efficiency with krypton is lower than with xenon, and that efficiency increases sharply with propellant mass flow rate. However, the data were limited in power and mass flow rate due to facility pumping limitations; the indicated tank pressure was typically over 5 x 10^{-5}-Torr. The high background pressure also introduced significant uncertainty into the measurements. Comprehensive comparisons of Kr and Xe have been performed the BHT-1500, SPT-100 and other thrusters.[25] All such comparisons show a significant performance penalty associated with the use of krypton.

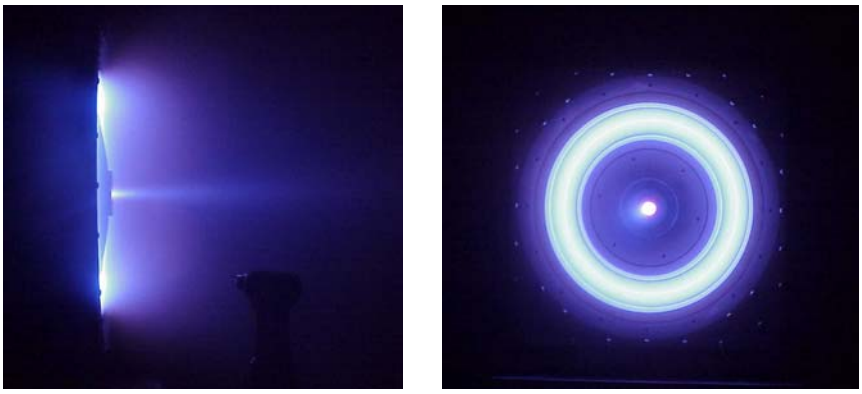

Figure 11. BHT-8000 operating on krypton propellant.

H. Iodine Performance

In 2012, the BHT-8000 was characterized with iodine propellant.[20] The thruster was fed by a high flow iodine feed system located outside the facility. The plume was neutralized by a Xe hollow cathode. Deep throttling of the thruster between 2-kW and 11-kW was demonstrated.

In general, specific thrust, specific impulse, and efficiency were very similar with iodine and xenon, reinforcing trends seen earlier with the BHT-200[20] and BHT-1000.[26] From Ref. 20, the measured performance with iodine at V_d =405-V, P =7.0-kW was T/P = 59-mN/kW +/- 1.2 mN/kW, I_{sp} =1940-s +/- 149-s, η = 56% +/- 5%. From this paper, the performance with Xe at V_d =405-V, P =6.2-kW was T/P = 56-mN/kW +/- 1.2 mN/kW, I_{sp} =2123-s +/- 72-s, and η = 58% +/- 3%. The best efficiency with iodine was measured at 500-V, where anode efficiency exceeded 66%. The indicated background pressures were comparable for xenon and iodine, but the actual background pressure may have been considerably lower for iodine. With respect to Xe, the calculated relative pressure gauge sensitivities for I and I_2 are 1.19-1.34 and 2.41, respectively.[27]

Discharge current oscillations were measured with a current probe and a digital oscilloscope. In this case, a capacitor bank shown in Figure 4 was not located in parallel with the discharge. Figure 12 shows predator-prey[28] or breathing mode[29] oscillations found when testing with iodine at V_d =500-V, I_d ~15-A. The frequency is 20 to 25-kHz. Typically, with xenon thrusters, the depth of the ionization oscillation varies widely with operating conditions, and no attempt was made to minimize the oscillations here.

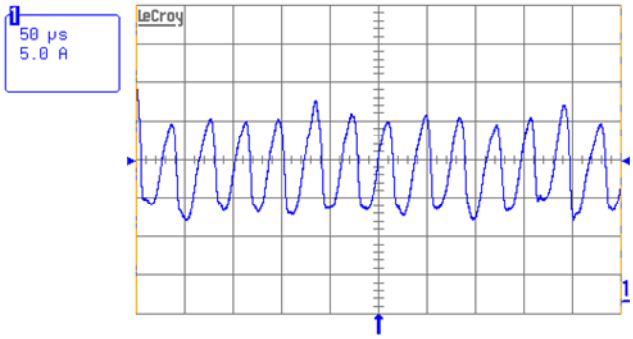

Figure 12. BHT-8000 discharge oscillations at V_d=500-V, I_d=15-A with I_2.

Plume current was sampled at a variety of operating conditions with a Faraday probe mounted upon a rotating arm at a distance of approximately half a meter from the center of the thruster exit plane. At V_d =300-V, I_d ~16-A, approximately 90% of the plume was included within 40 degrees. During this measurement, chamber pressure was below 5 x 10^{-5}-Torr (corrected for iodine). This assumes the background pressure is dominated by I_2.

IV. Discussion

A. Throttling and Propellant Utilization

The BHT-8000 has been tested at discharge potentials up to 700-V, yielding a specific impulse up to 3000-s. Factors influencing efficiency and specific impulse include the degree to which the neutral gas is converted to ion (the propellant utilization), the potential drop the ions experience, the ionization cost in terms of electron energy, and the divergence of the ion beam. The propellant density may be chosen to provide a balance between the erosion

rate and performance. In large thrusters, low propellant density can yield high propellant utilization. However, as thruster size decreases, the propellant density must increase to yield acceptable utilization. A significant fraction of the difference in maximum efficiency observed between the BHT-8000 and smaller thrusters of a similar design such as the BHT-1500[8] can be explained by the fact that the smaller thruster is not run at the "ideal" conditions; discharge power, which is roughly proportional to plasma density, is not scaled as D^{-1}, where D is thruster diameter and channel width is scaled proportionally.

B. Thruster Lifetime and Throughput

Busek projects a total available xenon throughput for the BHT-8000 of 1000-kg or more. This estimate is based upon scaling laws that related to the size of the channel and plasma density within it.

The lifetime of the thruster system must take into account the cathode. For short duration orbit raising emissions, even the 2000-h predicted for a 1250-C emitter will suffice. To support a 10,000-h mission, the emitter temperature should be maintained at 1150-C or below. For a 30,000-h mission, operating conditions should be maintained such that the emitter temperature is below 1100-C. Further work is required to correlate emitter temperatures with operating conditions and optimize cathode lifetime.

C. Flight System

In addition to the thruster and cathode, the flight BHT-8000 propulsion system includes four additional elements. These are the Power Processor Unit (PPU), Digital Control Interface Unit (DCIU), Xenon Feed System (XFS) and the propellant tank. The PPU distributes and regulates the power from the satellite power generation system to the thruster and support components. Contained within the PPU are back-to-back Zener diodes which provide electrical isolation from spacecraft common. The DCIU provides an abstraction layer between high-level spacecraft commands and thruster low-level actuation. It performs all control commands to operate and monitor the propulsion system**.** The XFS provides isolation, metering and active flow control of the propellant. All valves are operated through the PPU and commanded by the DCIU. Propellant flow is close-loop feedback controlled to provide constant thruster power operation The propellant tank provides high pressure gaseous storage of the propellant. Temperature regulation of the propellant is controlled by external heaters power directly from the spacecraft.

Busek's HET flight systems to date have used a fully integrated propulsion panel concept; the propellant tank is co-located on the propulsion panel. This method provides a turnkey system which simplifies spacecraft integration. Other than mechanical attachment of the panel to the spacecraft, the propulsion system requires only cable connections for propulsion system power and communications with the spacecraft. However, in systems which have

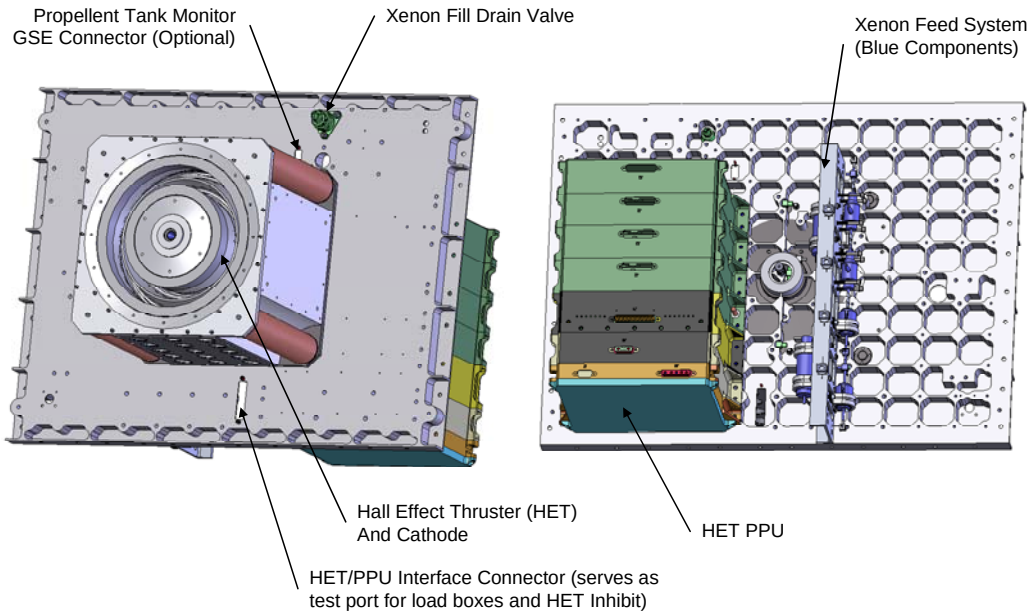

Figure 13. Notional layout of the BHT-8000 propulsion panel.

large propellant loading it may be advantageous to locate the tank remotely from the propulsion panel. Figure 13 shows a preliminary high power dual mode propulsion panel layout. The propellant tank is not shown. With xenon or krypton, the propellant would be stored at high pressure in a composite overwrapped pressure vessel (COPV) or possibly at cryogenic conditions. With iodine, the propellant would be stored as a dense solid at much lower pressure.

D. Mission Applications

Potential applications for the BHT-8000 include orbit maintenance, orbit raising, and interplanetary transfers.

The BHT-8000 is well sized for a 10-kW class all electric spacecraft. The thruster could provide both orbit-raising to geosynchronous orbit and on-orbit station-keeping.

The BHT-8000 could also maintain the orbit of the International Space Station (ISS), a mission which is currently accomplished by inefficient chemical propulsion. A NASA GRC study showed that thrust levels of 0.5-N to 1.0-N are required for reboosting the ISS under most conditions, and thrust greater than 1.5-N is required only for short times during the mission.[30] The study also determined that a xenon Hall thruster at 10-kW and 1770-s could reduce the chemical reboosting fuel by 50% or more.

The throttling ability of the BHT-8000 is important for interplanetary missions. Mars orbits at 1.52-AU, which reduces the solar constant to 43% of the value at Earth. Venus orbits at 0.72-AU, which increases the solar constant to 190% of the value at Earth. As a result the output power of a nominal 10-kW array varies between 4.3-kW and 19.1-kW as a spacecraft travels between these planets. The ability to throttle efficiently is even more important for missions beyond Mars.

Clustering the BHT-8000 would enable its use for much higher power missions, such as asteroid retrieval. In general, peak thruster efficiency increases monotonically with thruster size. However, as propellant utilization nears 100%, other considerations such as thruster redundancy may outweigh incremental efficiency gains. NASA thrusters have demonstrated power levels up to 100 kW.[31, 32] However, a cluster of BHT-8000 thrusters may be a more practical and reliable way to achieve 100-kW. A decade ago, the Air Force Research Laboratory (AFRL) initiated a program to cluster HETs. Sub-scale clusters of four were constructed using low-power Busek thrusters starting with the BHT-200 and proceeding to the BHT-600 (Figure 14). Performance and plume measurements showed no detrimental effects with clustering. In fact, clustering may slightly increase performance[33,34] and decrease plume divergence. [35,36] In general, however, the plume plasma density can be predicted by simple linear superposition of the contributions from individual thrusters.[37]

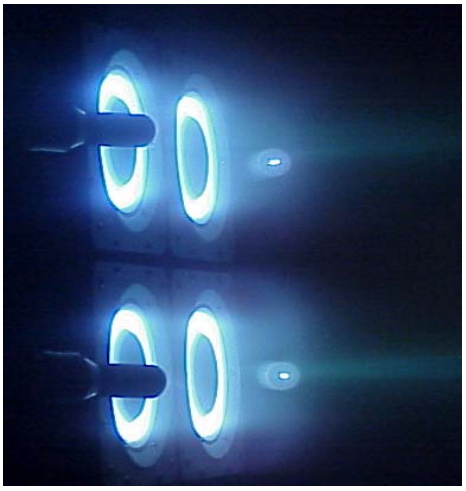

Figure 14. The BHT-600 has been clustered.

It is also possible to merge the magnetic circuits of neighboring thrusters in a cluster.[38] Sharing the magnetic circuit enables a significant reduction in overall mass with respect to a simple cluster.

When choosing between different propellants for a high throughput mission, system level considerations like storage density, pressure, and temperature should be taken into account. At typical storage conditions, e.g. 14-MPa and 50 degrees-C, the stored density of Xe is 1.6-kg/l. At the same conditions, Kr stores at just 0.5-kg/l. Iodine, on the other hand, stores in the solid phase, which has a density of 4.9-kg/l. Furthermore, iodine stores at very low pressure; the feed system pressure can me much less than one atmosphere. Even cryogenic Xe stores at only 60% of the density of iodine.

V. Conclusion

A breadboard high power Hall thruster was tested in multiple high vacuum simulated space environments, demonstrating TRL 5. The nominal power range of this thruster is 2-kW to 10-kW. The magnetic field in the channel is shaped into a high efficiency plasma lens by a magnetic shunt. The beam is neutralized by a 1.3-cm hollow cathode mounted along the thruster axis. This position has been proven to yield lower plume divergence than a cathode positioned distal to the discharge channel. The high voltage discharge is well isolated from the rest of the system by a custom propellant isolator.

A substantial body of performance data has been collected with a variety of propellants. Key performance metrics include thrust, power, efficiency and specific impulse. High efficiency while deep throttling was demonstrated. At nominal conditions, the thruster delivers half a Newton of thrust at 8-kW with a specific impulse of greater 1900-s. At high voltage, specific impulse as high as 3000-s was also measured. At low voltage, peak measured thrust to power was greater than 90 mN/kW. With xenon and iodine propellant, total thruster efficiency may exceed 60%. The use of krypton resulted in significantly lower efficiency. A numerical model predicts cathode lifetimes ranging from several thousand hours to many tens of thousands of hours, depending on the operating conditions. The estimated thruster xenon throughput is greater than 1000-kg.

Applications for this thruster include high power geostationary satellites, orbital tugs, and deep space missions. Examples destinations include high Earth orbits, the Moon, Mars, Venus, Near Earth Objects, and the asteroid belt. This thruster can also be clustered to 100-kW and above.

Acknowledgments

The BHT-8000 thruster was originally developed under the AFRL managed SBIR contract F04611-00-C-0018. The 1.3-cm cathode was developed under contract FA9300-06-C-1001. Iodine testing took place under NASA contract #NNX12CD99P. The cathode lifetime model was developed by WPI under subcontract.

References

[1]Janes, G., Dotson, J, and Wilson, T., "Momentum Transfer Through Magnetic Fields," *Proceedings of Third Symposium on Advanced Propulsion Concepts, Vol. 1*, Cincinnati, OH, October 2-4 1962, pp. 153-175, Gordon and Breach Science Publishers, New York, 1963.

[2]Meyerand, R., G., "Momentum Transfer Through the Electric Fields," *Proceedings of Third Symposium on Advanced Propulsion Concepts, Vol. 1*, Cincinnati, OH, 2-4 October, 1962, pp. 177-190, Gordon and Breach Science Publishers, New York, 1963.

[3]Seikel, G. R., "Generation of Thrust – Electromagnetic Thrusters," *Proceedings of the NASA-University Conference on the Science and Technology of Space Exploration*, Vol. 2, NASA SP-11, Nov. 1962, pp. 171-176.

[4]Morozov, A., I., "The Conceptual Development of Stationary Plasma Thrusters," *Plasma Physics Reports*, Vol. 29, No. 3, 2003, pp. 235-250.

[5]Monheiser, J., Hruby, V., Freeman, C., Connolly, W., and Pote, B., "Low-Power Hall Thruster System," in *Micropropulsion for Small Spacecraft*, ed. M. Micci and A. Ketsdever, *Progress in Astronautics and Aeronautics*, V. 187, 2000.

[6]Strange, N., Landau, D., Hofer, R., Snyder, J., Randolph, T., Campagnola, S., Szabo, J., and Pote, B., "Solar Electric Propulsion Gravity-Assist Tours for Jupiter Missions," 2012 AIAA/AAS Astrodynamics Specialists Conference, Minneapolis, MN, August 13-16, 2012.

[7]Pote, B., and Tedrake, R., "Performance of a High Specific Impulse Hall Thruster," *Proceedings of the 27th International Electric Propulsion Conference*, Electric Rocket Propulsion Society, IEPC Paper 01-35, Pasadena, CA, 2001.

[8]Szabo, J., Azziz, Y., "Characterization of a High Specific Impulse Xenon Hall Effect Thruster," *29th International Electric Propulsion Conference*, Electric Rocket Propulsion Society, IEPC Paper 05-324, Princeton University, 2005.

[9] Szabo, J., Pote, B., Hruby, V., Byrne, L., Tedrake, R., Kolencik, G., Kamhawi, H., Haag, T., "A Commercial One Newton Hall Effect Thruster for High Power In-Space Missions," *47th AIAA/ASME/SEA/ASEE Joint Propulsion Conference*, AIAA Paper 2011-6152, San Diego, CA, 31 July – 3 August 2011.

[10]Janes, G., Lowder, R., "Anomalous Electron Diffusion and Ion Acceleration in a Low-Density Plasma," *The Physics of Fluids*, Vol. 9., No. 6, pp. 1115-1123, June 1966.

[11]Pote, B., Hruby, V., Monheiser, J., "Performance of an 8 kW Hall Thruster," IEPC-99-080, *26th International Electric Propulsion Conference*, Electric Rocket Propulsion Society, Kitakyushu, Japan, October 17-21, 1999.

[12]Mankins, J., "Technology Readiness Levels: A White Paper", NASA, Office of Space Access and Technology, Advanced Concepts Office, April 1995.

[13] Hofer, R., Johnson, L., Goebel, D., Fitzgerald, D., "Effects of an Internally-Mounted Cathode on Hall Thruster Plume Properties," AIAA-2006-4482, *42nd AIAA/ASME/SAE/ASEE Joint Propulsion Conference & Exhibit*, Sacramento, CA, July 9-12, 2006.

[14]Hofer, R., Johnson, L., Goebel, D., Wirz, R.., "Effects of Internally Mounted Cathodes on Hall Thruster Plume Properties," IEEE Transactions on Plasma Science, Vol. 36, No. 5, October 2008.

[15]Busek Co. Inc., "Hall Field Plasma Accelerator with Inner and Outer Anode," U.S. Patent No. 6,075,321, 13 Jun 2000.

[16] Gavryshin, V., Kim, V., Kozlov, V., Maslennikov, N., "Physical and Technical Basis of the Modern SPT Development," Proceedings of the 24*th* International Electric Propulsion Conference, Electric Rocket Propulsion Society, Paper IEPC-1995-38, Moscow, Russia, September 1995.

[17]Morozov, A. I.; Kislov, A. Ya.; Zubkov, I. P., "Strong-current Plasma Accelerator with Closed Electron Drift," *Journal of Experimental and Theoretical Physics Letters*, Vol. 7, 1968, p.172-174.

[18]Morozov, A. I., Esipchuk, Yu. V., Kapulkin, A. M., Nevrovskii, V. A., Smirnov, V. A., "Effect of the Magnetic Field on a Closed-Electron-Drift Accelerator," *Soviet Physics – Technical Physics*, Vol. 17, No. 3, Sept. 1972, pp. 482-487.

[19]Haag, T., *Rev. Sci. Instrum*. 62, 1186, 1991.

[20] Szabo, J., Robin, M., Paintal, S., Pote, B., Hruby, V., Freeman, C., "Iodine Propellant Space Propulsion," *Proceedings of the 33rd International Electric Propulsion Conference*, Electric Rocket Propulsion Society, IEPC Paper 2013-311, *The George Washington University, USA*, October 6-10, 2013.

[21] Szabo, J., Pote, B., Paintal, S., Robin, M., Hillier, A., Branam, R., Huffman, R., "Performance Evaluation of an Iodine Vapor Hall Thruster", *AIAA Journal of Propulsion and Power*, Vol. 28, No. 4, July/August 2012, pp. 848-857. doi: 10.2514/1.B34291

[22]Wilson, E., *An Introduction to Scientific Research*, New York: McGraw Hill, 1952, pp. 272-274.

[23]Lipeles, R.A. and Kan, H.K.A., "Chemical Stability if Barium Calcium Aluminates Dispenser Cathode Impregnants," Appl. Surf. Sci, 16, 189-206, 1983.

[24]Wolten, G.M., "An Appraisal of the Ternary System BaO-CaO-Al2O3", SDTR-80-67, 1980.

[25]Nakles, M, Hargus, W., Delgado, J., and Corey, R., "A Performance and Plume Comparison of Xenon and Krypton Propellant on the SPT-100," 48th AIAA/ASME/SAE/ASEE Joint Propulsion Conference and Exhibit, AIAA paper 2012-4116, Atlanta, GA, 20 July – 01 August 2012.

[26]Szabo, J., Robin, M., Paintal, Pote, B., S., Hruby, V., "High Density Hall Thruster Propellant Investigations," *48th AIAA/ASME/SAE/ASEE Joint Propulsion Conference*, AIAA Paper 2012-3853, July 2012.

[27]Szabo, J., Robin, "Iodine Plasma Species Measurements in a Hall Effect Thruster Plume," *49th AIAA/ASME/SAE/ASEE Joint Propulsion Conference*, AIAA Paper 2013-4115, July 2013.

[28]Fife, M. Martinez-Sanchez, M., Szabo, J., "A Numerical Study of Low-Frequency Discharge Oscillations in Hall Thrusters," *33rd AIAA/ASME/ASE/ASEE Joint Propulsion Conference*, AIAA Paper 97-3052, Seattle, WA, July 97.

[29] Boeuf, J. P.; Garrigues, L. , *Journal of Applied Physics* , vol.84, no.7, pp.3541-3554, Oct 1998.

[30]Oleson, S., Benson, S., "Electric Propulsion for International Space Station Reboost: A Fresh Look," AIAA Paper 2001-3644, *37th AIAA/ASME/SEA/ASEE Joint Propulsion Conference and Exhibit*, Salt Lake City, Utah, July 8-11, 2001.

[31]Jankovsky, R., et al, "NASA's Hall Thruster Program 2002," AIAA-2002-3675, *38th AIAA/ASME/SEA/ASEE Joint Propulsion Conference*, Indianapolis, IN, July 7-10, 2002.

[32]Peterson, P., Jacobson, D., Manzella, D., and John, J., "The Performance and Wear Characterization of a High-Power High-Isp NASA Hall Thruster," AIAA-2005-4243, *31st AIAA/ASME/SEA/ASEE Joint Propulsion Conference and Exhibit*, Tucson, Arizona, July 10-13, 2005.

[33]Lobbia, R., Gallimore, A., "Performance Measurements from a Cluster of Four Hall Thrusters," IEPC-2007-177. *30th International Electric Propulsion Conferenc*e, Florence, Italy, Sep 17-20, 2007.

[34]Walker, M., Gallimore, A., "Performance Characteristics of a Cluster of 5-kW Laboratory Hall Thrusters," *Journal of Propulsion and Power*, Vol. 23, No. 1, pp. 35-43.

[35]Hargus, W., and Reed, G., "The Air Force Clustered Hall Thruster Program," AIAA-2002-3678, *38th AIAA/ASME/SEA/ASEE Joint Propulsion Conference*, Indianapolis, Indiana, July 7-10, 2002.

[36]Beal, B, Gallimore, A, and Hargus, W., "The Effects of Clustering Multiple Hall Thrusters on Plasma Plume Properties," AIAA 2003-5155, *39th AIAA/ASME/SEA/ASEE Joint Propulsion Conference*, Huntsville, AL, July 20-23, 2003.

[37]Beal, B., Gallimore, A., Haas, J., and Hargus, W., "Plume Properties in the Plume of a Hall Thruster Cluster," *Journal of Propulsion and Power*, Vol. 20, No. 6, 2004, pp. 985-991.

[38]Busek Co. Inc., "Hall Thruster with Shared Magnetic Structure," U.S. Patent No. 7,459,858, 2 Dec 2008.